

Controlling a Semiconductor Optical Amplifier Using a State-Space Model

Scott B. Kuntze, Lăcră Pavel, *Senior Member, IEEE*, and J. Stewart Aitchison, *Senior Member, IEEE*

Abstract—We derive nonlinear and linear state-space control models for a multichannel semiconductor optical amplifier. Verified against the governing partial differential equations through simulation, the linear model tracks modulations up to 20% qualitatively well. Linear feedback control is then employed to design two interchannel crosstalk suppressing systems, one using state feedback into the electronic drive current and the other using optical output feedback into an optical control channel; the controller designed with the linear model is seen to work well even with 100% modulations of the nonlinear system. This linear state-space model opens the way for further robust analysis, design and control of integrated active photonic circuits.

Index Terms—Feedback systems, gain control, linear approximation, optical crosstalk, optoelectronic control, power control, semiconductor optical amplifiers (SOAs), state space methods.

I. INTRODUCTION

ALTHOUGH not a perfect analog to the electronic transistor, the semiconductor optical amplifier (SOA) is a leading candidate for integrated photonic linear amplification and nonlinear switching. Depending on the electronic bias and power of the optical signal, linear amplification (through stimulated emission) [1], [2] and phase change (through gain saturation) [3], [4] are possible. SOAs are small and may be fully integrated into monolithic waveguide-based photonic circuits, and form the basis of active photonic circuitry [5]–[7].

While control theory provides a powerful set of analysis and design tools for photonic devices, its application to integrated SOAs is not yet widespread despite having been employed extensively for fiberline amplifier systems [8]–[10]. Although SOAs have been used in experimental systems with empirical optical [11], [12] and electronic [13]–[18] feedback control schemes, no analytical framework has been presented to date. Having a linear control model for SOAs would greatly facilitate design and analysis of integrated photonic control systems.

In this paper, we derive a general state-space model that captures the optoelectronic dynamics of an SOA at the expense of neglecting nonlinear optical effects. The goal of our derivation is to produce an input/output state-space model suitable for control applications that act on the inputs and outputs of the SOA. The dynamics responsible for the wide array of interesting amplification applications are still present in our model, even if some

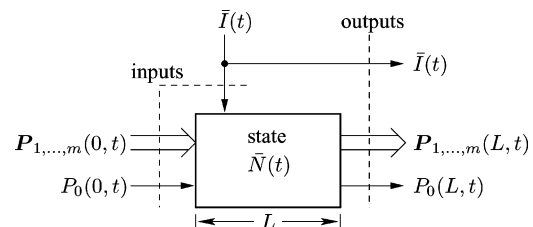


Fig. 1. Input/output control model of an SOA. Inputs: m lightwave data channels $P_{1,\dots,m}(0,t)$, auxiliary lightwave for SOA optical control $P_0(0,t)$, bias and modulation current $\bar{I}(t)$. Outputs: lightwave channels $P_{1,\dots,m}(L,t)$, auxiliary lightwave for SOA optical control $P_0(L,t)$, bias and modulation current $\bar{I}(t)$. State: length-averaged carrier concentration $\bar{N}(t)$.

of the nonlinear optical effects are neglected. We then derive a linear state-space model suitable for control analysis and design and use the linear model to design crosstalk suppressing systems in multichannel SOAs using electronic state and optical output feedback loops.

From an input/output perspective, a SOA is a multi-input/multi-output system, as shown in Fig. 1. The inputs are the electronic drive current $\bar{I}(t)$ and optical data and control channels $P(0,t)$. Measurable outputs are the electronic drive current and the optical channels after passing through the SOA, $\bar{I}(t)$ and $P(L,t)$ respectively. In Section II, we start from the governing partial differential equations and cast them in a nonlinear state-space form with the length-averaged population inversion carrier density $\bar{N}(t)$ as the state variable.

Linearizing the state equations about preset input conditions yields a linear model of the SOA (Section III). This linear model is verified against the original partial differential equations under various simulated input conditions.

In Section IV, a state feedback controller is implemented to eliminate interchannel crosstalk by negative feedback into the electrical drive current. An output feedback controller is then implemented to suppress crosstalk by using the optical outputs to drive a regulating optical control channel.

These derivations and demonstrations show that control theory provides systematic methods for designing and regulating integrated photonic amplifiers (Section V).

II. NONLINEAR STATE-SPACE MODEL

In this section we start from the SOA governing equations and derive a dynamic state-space model (a set of first-order ordinary differential equations) that is suitable for linearization and control.

Manuscript received April 11, 2006; revised September 20, 2006. The work of S. B. Kuntze was supported in part by a NSERC Canadian Graduate Scholarship.

The authors are with The Edward S. Rogers Sr. Department of Electrical and Computer Engineering, University of Toronto, Toronto, ON M5S 3G4, Canada (e-mail: scott.kuntze@utoronto.ca).

Digital Object Identifier 10.1109/JQE.2006.887176

A. Governing Equations

The governing equations for a two-level multichannel SOA consist of an optical power propagation equation

$$\frac{\partial P_i(z, t)}{\partial z} = g_i(N(z, t), \mathbf{P}(z, t)) P_i(z, t) - \alpha_i P_i(z, t) \quad (1)$$

and an electronic carrier rate equation

$$\frac{\partial N(z, t)}{\partial t} = \frac{I(z, t)}{qV} - R(N, t) - \frac{1}{A} \sum_{i=0}^m \frac{g_i(N(z, t), \mathbf{P}(z, t))}{\hbar\omega_i} P_i(z, t). \quad (2)$$

In these equations for channel i , $P_i(z, t)$ is the instantaneous optical power with $\mathbf{P}(z, t) = (P_0(z, t), \dots, P_m(z, t))$, $N(z, t)$ the instantaneous population inversion carrier density, $g_i(N(z, t), \mathbf{P}(z, t))$ the stimulated optical gain, α_i the optical loss from scattering and free carrier absorption, $I(z, t)$ the injection current, q the electronic unit charge, V and A the interaction volume and transverse area, $R(N, t)$ the recombination rates (excluding stimulated emission), and ω_i the optical carrier frequency. The SOA is assumed time-invariant and homogeneous along its length.

This SOA model handles multiple optical channels by indexing parameters on a channel-by-channel basis. We adopt the convention that there are m optical data channels indexed $1, \dots, m$, and one auxiliary optical control channel numbered 0, as shown in Fig. 1. Typically with this convention, each indexed parameter in (1) and (2) is constant over the given channel's bandwidth, but the parameters can be unique for every channel; because each channel is indexed to a single central frequency ω_i , interchannel spectral overlap is ignored, but there is no restriction on maximum channel bandwidth and interchannel crosstalk is still possible due to the coupling through the common inversion carrier density (2). If, however, spectral overlap and intra-channel variations must be incorporated, sets of indexes can be assigned to each channel and the parameters varied piecewise over the channel bandwidths.

B. Gain

The form of the gain function has a profound impact on the algebra needed to create a state-space model. For any unknown time-varying quantity, we must have an analytical rate equation so that the unknown quantity can be made a state of the system; however, not all the required rate equations are convenient or available.

We assume that local gain g_i depends on the local charge carrier density N , but not the local optical powers \mathbf{P} . While slightly restrictive, this assumption is particularly useful because it allows us to obtain a closed-form state equation and is still general enough to model nonlinear gain. Compressive gains that involve optical powers lead to output differential equations (1) without suitable closed-form solutions if N depends on z ; if N is taken to be z -independent *a priori*, it is possible to find an output solution as shown in the Appendix, but the explicit solution exists only in the single-channel case and the algebraic forms in the subsequent derivation of the state-space model are far too cumbersome to reproduce in the present paper.

Furthermore, because our goal is to produce an input/output model, we will integrate the gain over the length of the SOA

[19]. Therefore, we take the charge carrier density N to be constant over the length of the device, $N(z, t) = N(t)$, because integrating optical output relation in the following section reduces the SOA to a lumped element and averages the internal spatial information to a single value $N(t)$.

With these assumptions, gain for each channel i can be modeled linearly [20]

$$g_i(N, t) = \Gamma_i a_i (N(t) - N_{\text{tr}, i}) \quad (3)$$

or logarithmically

$$g_i(N, t) = \Gamma_i a_i \ln \left(\frac{N(t)}{N_{\text{tr}, i}} \right) \quad (4)$$

where Γ is the modal confinement factor, a is the differential gain, and N_{tr} is the transparency carrier density.

C. Output Relations

1) *Electrical Domain*: The drive current is not necessarily the instantaneous current seen by the SOA because the power source and SOA may have parasitic resistance, capacitance and inductance. Although augmenting the model with linear circuit equations is straightforward, for simplicity we ignore the dynamics of any electronic drive circuitry and assume we can measure and adjust the electrical drive current $\bar{I}(t)$ directly. Hence, the electrical input and output are equal.

2) *Optical Domain*: To relate the optical outputs at $z = L$ to the inputs at $z = 0$ we separate variables of the propagation equation (1), integrate and normalize on $[0, z]$, and solve for the optical power at location z in terms of the input power

$$P_i(z, t) = P_i(0, t) e^{[g_i(N, t) - \alpha_i]z}. \quad (5)$$

At the end of the device the optical output is

$$P_i(L, t) = P_i(0, t) e^{[g_i(N, t) - \alpha_i]L}. \quad (6)$$

D. State Update Equation

Integrating the multichannel rate (2) on $z \in [0, L]$ and normalizing by $1/L$ we have

$$\frac{dN(t)}{dt} = \frac{\bar{I}(t)}{qV} - R(N, t) - \frac{1}{A} \sum_{i=0}^m \frac{g_i(N, t) \bar{P}_i(t)}{\hbar\omega_i} \quad (7)$$

where Leibnitz's Rule has been employed to interchange the time derivative and the spatial definite integral in (7) (for a proof, see [21, p. 266]). In (7) we have defined

$$\bar{I}(t) \triangleq \frac{1}{L} \int_0^L I(z, t) \partial z \quad (8)$$

and

$$\bar{P}_i(t) \triangleq \frac{1}{L} \int_0^L P_i(z, t) \partial z. \quad (9)$$

Substituting (5) into (9) gives

$$\bar{P}_i(t) = \frac{P_i(0, t) [e^{[g_i(N, t) - \alpha_i]L} - 1]}{[g_i(N, t) - \alpha_i]L}. \quad (10)$$

Because N is assumed to be spatially invariant

$$\bar{N}(t) \triangleq \frac{1}{L} \int_0^L N(t) dz \quad (11)$$

is simply given by $N(t)$ everywhere and we omit the overscript bar $\bar{N}(t) = N(t)$. Substituting (10) into the rate equation (7) we get

$$\frac{dN(t)}{dt} = \frac{\bar{I}(t)}{qV} - R(N, t) - \frac{1}{V} \sum_{i=0}^m \frac{g_i(N, t) P_i(0, t) [e^{[g_i(N, t) - \alpha_i]L} - 1]}{\hbar\omega_i [g_i(N, t) - \alpha_i]} \quad (12)$$

which represents the general nonlinear state equation for any recombination $R(N, t)$ and any set of gains $\mathbf{g}(N, t)$. This state update equation is nonlinear in the carrier concentration but affine in both electrical and optical inputs (i.e., the inputs can be factored out algebraically).

E. Nonlinear Control Form Summary

We define the state variable as

$$x(t) \triangleq \bar{N}(t). \quad (13)$$

and the electrical and optical inputs as

$$u_e(t) \triangleq \bar{I}(t) \quad (14)$$

$$\mathbf{u}_o(t) \triangleq \mathbf{P}(0, t). \quad (15)$$

Finally, we define the electrical and optical outputs as

$$y_e(t) \triangleq \bar{I}(t) \quad (16)$$

$$\mathbf{y}_o(t) \triangleq \mathbf{P}(L, t). \quad (17)$$

Concatenating the electronic and optical domains yields total input and output vectors defined by

$$\mathbf{u}(t) \triangleq \begin{bmatrix} u_e(t) \\ \mathbf{u}_o(t) \end{bmatrix} \quad (18)$$

$$\mathbf{y}(t) \triangleq \begin{bmatrix} y_e(t) \\ \mathbf{y}_o(t) \end{bmatrix}. \quad (19)$$

The nonlinear system state update (12) can then be written as

$$\frac{d}{dt} x(t) = \frac{u_e(t)}{qV} - R(x, t) - \frac{1}{V} \sum_{i=0}^m \frac{g_i(x, t) [e^{[g_i(x, t) - \alpha_i]L} - 1]}{\hbar\omega_i [g_i(x, t) - \alpha_i]} u_{o,i}(t) \quad (20)$$

with nonlinear output relation (from (6))

$$\mathbf{y}(t) = \begin{bmatrix} 1 & e^{[g_0(x, t) - \alpha_0]L} & \dots & e^{[g_m(x, t) - \alpha_m]L} \end{bmatrix} \mathbf{u}(t). \quad (21)$$

We have now converted the partial differential SOA (1) and (2) into a state-space form suitable for linearizing. This nonlinear

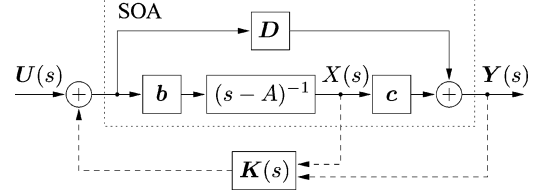


Fig. 2. Linear model ($A, \mathbf{b}, \mathbf{c}, \mathbf{D}$) of a SOA used in the control designs. Either the state $X(s)$ or output $Y(s)$ may be fed back to the input $U(s)$ through controller $\mathbf{K}(s)$. The control simulations are applied to the nonlinear SOA model.

model (20) and (21) was verified with the commercial photonic systems simulator VPI [22].

III. LINEAR STATE-SPACE MODEL

The general state-space dynamic model (20) and (21) is nonlinear. We seek the linearized model ($A, \mathbf{b}, \mathbf{c}, \mathbf{D}$) of the form

$$\frac{d}{dt} \delta x(t) = A \delta x(t) + \mathbf{b} \delta \mathbf{u}(t) \quad (22)$$

$$\delta \mathbf{y} = \mathbf{c} \delta x(t) + \mathbf{D} \delta \mathbf{u}(t) \quad (23)$$

about equilibria x_0, \mathbf{u}_0 , and \mathbf{y}_0 , and for which $x(t) = x_0 + \delta x(t)$, $\mathbf{u}(t) = \mathbf{u}_0 + \delta \mathbf{u}(t)$, and $\mathbf{y}(t) = \mathbf{y}_0 + \delta \mathbf{y}(t)$. The equilibrium point x_0 is found numerically by setting $\dot{x}(t) = 0$ for a given \mathbf{u}_0 in (20). The output equilibrium points are simply $\mathbf{y}_0 = \mathbf{y}(x_0, \mathbf{u}_0)$ using (21). This model is depicted in Fig. 2 where the variables have been transformed to the Laplace domain to allow straightforward block multiplication ($\mathbf{U}(s) = \mathcal{L}\{\mathbf{u}(t)\}$, $X(s) = \mathcal{L}\{x(t)\}$, $\mathbf{Y}(s) = \mathcal{L}\{\mathbf{y}(t)\}$).

Linearizing (20) and (21) about an arbitrary equilibrium point (x_0, \mathbf{u}_0) [23] we compute for general gain $\mathbf{g}(N, t)$

$$A = - \left. \frac{\partial R(x, t)}{\partial x} \right|_{x_0} - \sum_{i=0}^m \frac{u_{o,i,0}}{V \hbar \omega_i [g_i(x_0) - \alpha_i]} \times \left([1 + g_i(x_0)L] e^{[g_i(x_0) - \alpha_i]L} - 1 \right) \frac{g_i(x_0) (e^{[g_i(x_0) - \alpha_i]L} - 1)}{g_i(x_0) - \alpha_i} \left. \frac{\partial g_i(x)}{\partial x} \right|_{x_0} \quad (24a)$$

$$\mathbf{b}^T = \begin{bmatrix} 1/qV \\ \frac{g_0(x_0)(1 - e^{[g_0(x_0) - \alpha_0]L})}{V \hbar \omega [g(x_0) - \alpha_0]} \\ \vdots \\ \frac{g_m(x_0)(1 - e^{[g_m(x_0) - \alpha_m]L})}{V \hbar \omega [g(x_0) - \alpha_m]} \end{bmatrix} \quad (24b)$$

$$\mathbf{c} = \begin{bmatrix} 0 \\ u_{o,0,0} L e^{[g_0(x_0) - \alpha_0]L} \left. \frac{\partial g_0(x)}{\partial x} \right|_{x_0} \\ \vdots \\ u_{o,m,0} L e^{[g_m(x_0) - \alpha_m]L} \left. \frac{\partial g_m(x)}{\partial x} \right|_{x_0} \end{bmatrix} \quad (24c)$$

$$\mathbf{D} = \begin{bmatrix} 1 & 0 & & \\ 0 & e^{[g_0(x_0) - \alpha_0]L} & & 0 \text{ elsewhere} \\ & & \ddots & \\ 0 & & & e^{[g_m(x_0) - \alpha_m]L} \end{bmatrix}. \quad (24d)$$

Hence, we have obtained a time-invariant SOA model that is linear in the state and inputs.

TABLE I
PARAMETERS FOR SIMULATIONS (ALL CHANNELS)

Parameter	Symbol	Value	Unit
Length	L	500	μm
Active width	W	3	μm
Active height	H	80	nm
Confinement	Γ	0.15	—
Waveguide loss	α	40	cm^{-1}
Differential gain	a	2.78×10^{-20}	m^2
Transparency carrier density	N_{tr}	1.4×10^{18}	cm^{-3}
Linear recombination	R_A	1.43×10^8	s^{-1}
Bimolecular recombination	R_B	10^{-16}	m^3s^{-1}
Auger recombination	R_C	3×10^{-41}	m^6s^{-1}

To verify the linear model ($A, \mathbf{b}, \mathbf{c}, \mathbf{D}$), we compare its response to the response of the nonlinear system (20) and (21) numerically integrated in time. For example we consider two identical optical channels with linear gain (3) and recombination in the form of $R(N, t) = R_A N + R_B N^2 + R_C N^3$ [20]. We use the parameters of [22] listed in Table I with $\lambda_0 = 1550$ nm for both channels throughout. Taking equilibrium inputs as

$$\mathbf{u}_0^T = [150 \text{ mA} \quad 0.6 \text{ mW} \quad 1 \text{ mW}] \quad (25)$$

we calculate the equilibrium state

$$x_0 = 3.891875 \times 10^{24} \text{ m}^{-3} \quad (26)$$

and linear coefficients

$$A = -9.9033 \times 10^9 \text{ s}^{-1} \quad (27a)$$

$$\mathbf{b}^T = \begin{bmatrix} 5.2013 \text{ A}^{-1} \\ -247.64 \text{ W}^{-1} \\ -247.64 \text{ W}^{-1} \end{bmatrix} \times 10^{34} \text{ m}^{-3} \cdot \text{s}^{-1} \quad (27b)$$

$$\mathbf{c} = \begin{bmatrix} 0 \text{ A} \\ 3.0554 \text{ W} \\ 5.0924 \text{ W} \end{bmatrix} \times 10^{-26} \text{ m}^3 \cdot \text{s} \quad (27c)$$

$$\mathbf{D} = \begin{bmatrix} 1 & 0 & 0 \\ 0 & 24.42384 & 0 \\ 0 & 0 & 24.42384 \end{bmatrix}. \quad (27d)$$

Fig. 3 shows simulation results comparing the nonlinear model with the linearized model for 20% input step modulations: (a) shows the optical outputs and (b) shows the state due to modulation of the optical inputs (c) and electrical input (d). For each modulation the linear model follows the nonlinear one very closely in terms of transient and steady-state responses. Cross-talk is evident between the optical channels during optical modulation because the channels are coupled together through the state (i.e., each optical channel draws from the common population inversion carrier density).

Some deviation is noticeable for larger modulation (typically in excess of 20% modulation from equilibrium) but overall performance is qualitatively good. Quantitative agreement is difficult to generalize because it depends on the relative nonlinearity of the dynamics in (20) and (21), although specific deviations can be calculated either by subtracting the linear and

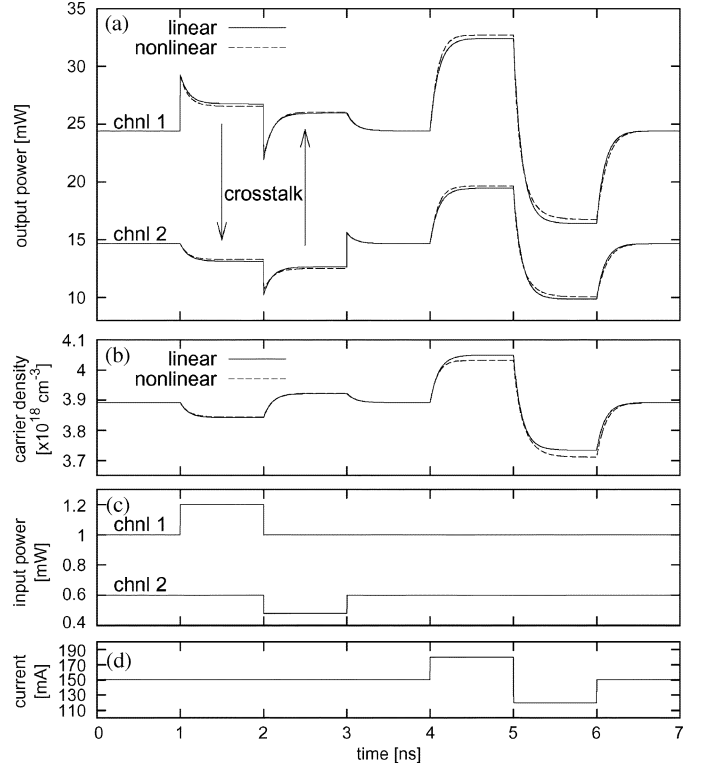


Fig. 3. Verification of the linear model equations (22)–(24) with nonlinear model equations (20) and (21) by direct numerical integration. (a) Optical output and (b) state modulation due to (c) optical input modulation and (d) electrical input modulation. All step modulations are 20% of nominal values. Channel crosstalk is evident during optical modulation.

nonlinear models, or by calculating the second-order differential terms and weighing them against the linear terms (24). It is up to the designer how much error is permissible in a given application. In fact, the output feedback controller in Section IV works well for 100% modulation because of the action of the feedback. For applications where there are several operating points, a controller may schedule (switch) its gain based on the linear model evaluated at several different sets of pre-calculated equilibria.

IV. FEEDBACK CONTROL

In this section we employ our linear model ($A, \mathbf{b}, \mathbf{c}, \mathbf{D}$) to design two SOA control schemes to suppress interchannel crosstalk: electronic state feedback and optical output feedback. For both cases we use constant feedback $\mathbf{K}(s) = \mathbf{k}$ for simplicity in demonstrating the concepts, although the controller could certainly be generalized to include dynamic terms (differentiators and integrators) to improve transient characteristics and eliminate steady-state errors. The linear model greatly simplifies the controller design and the controller is then applied to the *nonlinear* SOA model (20) and (21) to verify the performance.

A. State Feedback: Suppressing Cross-Talk Electronically

With constant negative state feedback, the state is scaled and fed back into the SOA as illustrated in the block diagram Fig. 2

by taking the branch from the state $X(s)$. Closing the loop from state to input yields the new state update equation

$$\frac{d}{dt}\delta x(t) = [A - \mathbf{bk}]\delta x(t) + \mathbf{b}\delta u(t) \quad (28)$$

and new output relation

$$\delta \mathbf{y}(t) = (\mathbf{c} - \mathbf{Dk})\delta x(t) + \mathbf{D}\delta u(t) \quad (29)$$

where \mathbf{k} is a constant $(m+2) \times 1$ column vector that describes how the state is scaled and fed back into each input (one electrical and $m+1$ optical inputs).

State dynamics in the frequency domain are given by

$$sX(s) - x(0) = AX(s) \Rightarrow X(s) = (s - A)^{-1}x(0) \quad (30)$$

so the SOA has a single pole at $s = A$. Pushing the pole further negative will cause the state to converge more quickly to x_0 , thereby reducing excursions in the state due to the inputs. Letting the desired pole location be s' we calculate the control gains by solving for \mathbf{k} in $s' - A + \mathbf{bk} = 0$. There is some flexibility in choosing a pole location that achieves the control objective (suppressing crosstalk) with reasonable controller gain.

Consider the SOA system verified in Section III, again with linear gain (3), recombination $R(N, t) = R_A N + R_B N^2 + R_C N^3$, and two identical optical channels. We employ feedback from the state x into the electrical drive current u_e , so $k_2 = k_3 = 0$. For illustration we choose $s' = 5A$ and calculate

$$k_1 = \frac{A - s'}{b_1} = 7.6161 \times 10^{-25} \text{ m}^3 \text{ A}. \quad (31)$$

Fig. 4 shows that state feedback into the electrical drive current (d) suppresses crosstalk between optical channels (a) due to optical input modulation (c). The negative feedback reduces fluctuations in the state Fig. 4(b): as optical channel 1 steps up, the state wants to step down as carriers are depleted by stimulated emission, but this step down in state is converted into a step up in drive current, thereby refilling the population inversion. Because the population inversion is held relatively constant, the channels decouple and interchannel crosstalk collapses. With the decoupling, modulated channels receive better steady-state gain and better transient response.

Greater controller gain k_1 yields better output performance at the expense of greater and faster swings in the drive current. To illustrate, let the drive current seen by the SOA be $\mu_1(t)$, defined by

$$\mu_1(t) = u_1(t) - k_1 x(t) \quad (32)$$

from Fig. 2. Using the Laplace transform of (28) to find the state $x(t)$, setting $u_1(t)$ to a constant reference, and assuming that the total change in optical input $u_{\text{opt}}(t)$ is a step function with

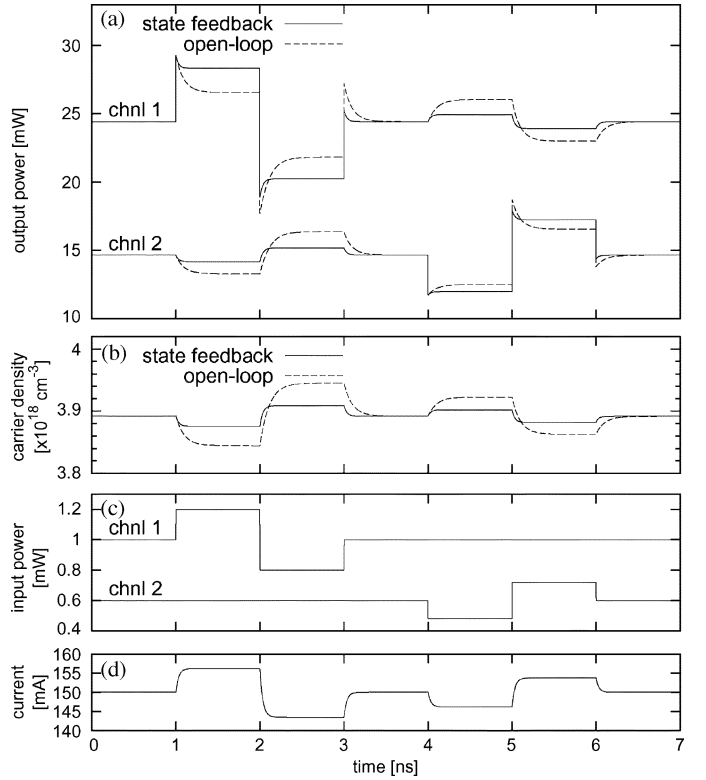


Fig. 4. Constant negative state feedback applied to the electrical input ($\mathbf{k} = [7.6161 \times 10^{-25} \text{ m}^3 \text{ A } 0 \ 0]$) of the nonlinear model equations (20) and (21). Crosstalk in the outputs (a) is essentially eliminated because the state (b) is forced to be constant by feedback into the drive current (d). (c) Optical inputs modulated with 20% steps from equilibrium.

amplitude Δu_{opt} , the magnitude of drive current change called for by the controller is given by

$$\Delta \mu_1(t) = \frac{1 - e^{-(|A| + |b_1 k_1|)t}}{|b_1| + |A/k_1|} \left(\sum_{i=2}^m b_i \right) \Delta u_{\text{opt}}. \quad (33)$$

As the controller gain k_1 increases, the denominator of $\Delta \mu_1(t)$ decreases, thus $\Delta \mu_1(t)$ increases with k_1 and so greater drive current swings are required as the transient response fades. The time constant of the exponential transient $\tau = (|A| + |b_1 k_1|)^{-1}$ decreases as k_1 increases, and so faster drive current swings are required.

B. Output Feedback: Suppressing Cross-Talk Optically

Measuring the state—the average population inversion along the length of the SOA—is difficult in real time. Although an observer circuit could be constructed in parallel to estimate the state, the outputs are much easier to measure physically and so we now consider direct output feedback.

Tapping the outputs and feeding them back into the plant yields constant output feedback, illustrated in the system block diagram Fig. 2 taking the branch that feeds the output $\mathbf{Y}(s)$ back to the input through constant controller $\mathbf{K}(s) = \mathbf{K}$. Optical outputs are readily available and easily measured, so this control scheme lends itself to a straightforward implementation.

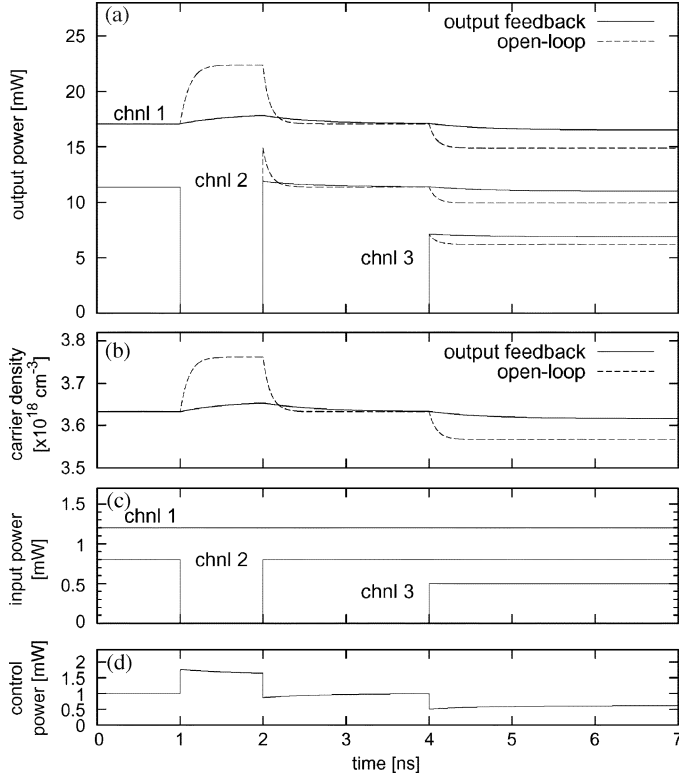


Fig. 5. Optical constant output feedback applied from the sum of optical outputs into the optical control channel of the nonlinear model equations (20) and (21). Interchannel crosstalk in the optical outputs (a) from the optical inputs (c) is suppressed. The controlled optical input (d) holds the state (b) relatively constant by negative feedback action. Optical modulations are 100% steps from equilibrium.

Closing the loop from output to input yields the state update equation

$$\frac{d}{dt}\delta x(t) = [A + \mathbf{b}\mathbf{K}(\mathbf{I} - \mathbf{D}\mathbf{K})^{-1}\mathbf{c}] \delta x(t) + \mathbf{b}[\mathbf{I} + \mathbf{K}(\mathbf{I} - \mathbf{D}\mathbf{K})^{-1}\mathbf{D}] \delta \mathbf{u}(t) \quad (34)$$

and output relation

$$\delta \mathbf{y}(t) = (\mathbf{I} - \mathbf{D}\mathbf{K})^{-1}\mathbf{c}\delta x(t) + (\mathbf{I} - \mathbf{D}\mathbf{K})^{-1}\mathbf{D}\delta \mathbf{u}(t) \quad (35)$$

where \mathbf{K} is a constant $(m+2) \times (m+2)$ matrix that scales each output (across the columns) into each input (across the rows).

Consider the same SOA system from above, and add a third data channel and a dedicated optical control channel with equilibrium inputs now set to

$$\mathbf{u}_0^T = [150 \text{ mA} \quad 1.0 \text{ mW} \quad 1.2 \text{ mW} \quad 0.8 \text{ mW} \quad 0.0 \text{ mW}]. \quad (36)$$

The terms in \mathbf{u}_0^T are the drive current, optical power in the control channel, and optical powers in data channels 1–3 with channel 3 initially dark. The linear coefficients (24) are re-evaluated given these new input equilibria.

To sum the optical outputs and loop their total back into the control optical input with moderate negative scaling, we set

$$\mathbf{K} = -2 \begin{bmatrix} 0 & 0 & 0 & 0 & 0 \\ 0 & 1 & 1 & 1 & 1 \\ 0 & 0 & 0 & 0 & 0 \\ 0 & 0 & 0 & 0 & 0 \\ 0 & 0 & 0 & 0 & 0 \end{bmatrix}. \quad (37)$$

Fig. 5 shows the results of constant output feedback into the optical control channel. When channel 2 turns off at $t = 1$ ns (c), crosstalk into channel 1 is suppressed (a) because the control channel responds (d) to keep the state constant (b) by keeping the total input optical power constant at the preset equilibrium value. When channel 2 returns at $t = 2$ ns, the transient power spike in the open loop is suppressed by the feedback action. The control channel adjusts again when channel 3 comes online at $t = 4$ ns to suppress crosstalk into the other channels and improve the gain of all three data channels. The control channel must be set at sufficiently high power to accommodate the total power of all added or increased data channels.

V. CONCLUSION

We have cast the SOA governing equations in a state-space form and derived a linear multichannel control model. The model can accommodate any gain function of the form $g(N(t))$. Constant state feedback and output controllers were employed to suppress interchannel crosstalk electronically and optically during multichannel amplification. The model can be extended to include models for the electronic drive circuitry and more advanced robust design and control.

APPENDIX

In the single-channel case, let $N(z, t) = N(t)$ so that carrier density is independent of position z . With rational gain compression $[1 + \epsilon P(z, t)]^{-1}$, the propagation equation becomes

$$\frac{\partial P(z, t)}{\partial z} = g(N, t) \frac{P(z, t)}{1 + \epsilon P(z, t)} - \alpha P(z, t) \quad (38)$$

which does not have an analytical closed-form solution. With polynomial gain compression $1 - \epsilon P(z, t)$, the propagation equation becomes

$$\frac{\partial P(z, t)}{\partial z} = g(N, t) P(z, t) [1 - \epsilon P(z, t)] - \alpha P(z, t) \quad (39)$$

which has the solution

$$P(z, t) = P(0, t) (g(N, t) - \alpha) \left[(g(N, t) - \alpha) e^{-[g(N, t) - \alpha]z} + \epsilon (1 - e^{-[g(N, t) - \alpha]z}) g(N, t) P(0, t) \right]^{-1}. \quad (40)$$

Note that we obtain the output relation (5) when $\epsilon = 0$ provided $g(N, t) \neq \alpha$ in the single-channel case.

Substituting (40) into the carrier rate (2) and then integrating with respect to z yields extremely large expressions, because both P and P^2 must be integrated with respect to z . The algebraic steps are possible and new linear coefficients ($A, \mathbf{b}, \mathbf{c}, \mathbf{D}$) can be generated, but they are too lengthy to report here.

REFERENCES

- [1] K. D. LaViolette, "The use of semiconductor-optical-amplifiers for long optical links in the CATV upstream optical network," *IEEE Photon. Technol. Lett.*, vol. 10, no. 8, pp. 1165–1167, Aug. 1998.
- [2] C. Brisson, S. Chandrasekhar, G. Raybon, and K. F. Dreyer, "Experimental investigation of SOAs for linear amplification in 40 Gb/s transmission systems," in *Proc. Opt. Fiber Commun. Conf.*, 2002, pp. 343–345.
- [3] J. M. Tang, P. S. Spencer, and K. A. Shore, "Influence of fast gain depletion on the dynamic response of TOAD's," *IEEE J. Lightw. Technol.*, vol. 16, no. 1, pp. 86–91, Jan. 1998.
- [4] L. Schares, C. Schubert, C. Schmidt, H. G. Weber, L. Occhi, and G. Guekos, "Phase dynamics of semiconductor optical amplifiers at 10–40 GHz," *IEEE J. Quantum Electron.*, vol. 39, no. 11, pp. 1394–1408, Nov. 2003.
- [5] R. Hess, M. Caraccia-Gross, W. Vogt, E. Gamper, P. A. Besse, M. Duell, E. Gini, H. Melchior, B. Mikkelsen, M. Vaa, K. S. Jepsen, K. E. Stubkjaer, and S. Bouchoule, "All-optical demultiplexing of 80 to 10 Gb/s signals with monolithic integrated high-performance Mach-Zehnder interferometer," *IEEE Photon. Technol. Lett.*, vol. 10, no. 1, pp. 165–167, Jan. 1998.
- [6] P. V. Studenkov, M. R. Gokhale, J. Wei, W. Lin, I. Glesk, P. R. Prucnal, and S. R. Forrest, "Monolithic integration of an all-optical Mach-Zehnder demultiplexer using an asymmetric twin-waveguide structure," *IEEE Photon. Technol. Lett.*, vol. 13, no. 6, pp. 600–602, Jun. 2001.
- [7] V. M. Menon, W. Tong, and S. R. Forrest, "Control of quality factor and critical coupling in microring resonators through integration of a semiconductor optical amplifier," *IEEE Photon. Technol. Lett.*, vol. 16, no. 5, pp. 1343–1345, May 2004.
- [8] D. H. Richards, J. L. Jackel, and M. A. Ali, "A theoretical investigation of dynamic all-optical automatic gain control in multichannel EDFAs and EDFA cascades," *IEEE J. Sel. Topics Quantum Electron.*, vol. 3, no. 4, pp. 1027–1036, Aug. 1997.
- [9] Y. Taing and L. Pavel, " H_∞ optimal control design for time dependent tones within erbium-doped fiber amplifiers," in *Proc. IEEE IECON*, Nov. 2005, vol. 32, pp. 13–17.
- [10] M. Ding and L. Pavel, "Gain scheduling control design of an erbium-doped fibre amplifier by pump compensation," in *Proc. IEEE Conf. Contr. Appl.*, Aug. 2005, pp. 510–516.
- [11] I. Monfils, C. Ito, and J. C. Cartledge, "10 Gbit/s all-optical clock recovery using three-section DFB laser with optical feedback," *Electron. Lett.*, vol. 41, no. 24, pp. 1342–1343, Nov. 2005.
- [12] N. Pleros, C. Bintjas, G. Theophilopoulos, K. Yiannopoulos, S. Sygletos, and H. Avramopoulos, "Multiwavelength and power equalized SOA laser sources," *IEEE Photon. Technol. Lett.*, vol. 14, no. 5, pp. 693–695, May 2002.
- [13] X. Zhao, J. H. Chen, and F. S. Choa, "Performance analysis of gain-clamped semiconductor optical amplifiers using different clamping schemes," in *Proc. Optoelectron. Microelectron. Mater. Devices Conf.*, 1997, vol. 1, pp. 337–338.
- [14] L. F. Tiemeijer, S. Walczyk, A. J. M. Verboven, G. N. van den Hovenand, P. J. A. Thijs, T. van Dongen, J. J. M. Binsma, and E. J. Jansen, "High-gain 1310 nm semiconductor optical amplifier modules with a built-in amplified signal monitor for optical gain control," *IEEE Photon. Technol. Lett.*, vol. 9, no. 3, pp. 309–311, Mar. 1997.
- [15] A. Wonfor, S. Yu, R. V. Penty, and I. H. White, "Novel constant output power control of a semiconductor optical amplifier based switch," in *Proc. CLEO*, 2001, p. 43.
- [16] E. D. Park, T. J. Croeze, P. J. Delfyett, Jr., A. Braun, and J. Abeles, "16 × 10 GHz multiwavelength modelocked InGaAsP laser with closed loop spectral control," in *Proc. CLEO*, 2002, p. 413.
- [17] M. L. Majewski, A. D. Rakic, L. A. Coldren, and Y. Akulova, "Integrated semiconductor optical amplifiers for wavelength monitoring and power control in tunable sampled-grating DBR lasers," in *Proc. Optoelec. Microelec. Mater. Devices*, 2002, pp. 121–124.
- [18] H. Wessing, B. Sorensen, B. Lavigne, E. Balmezfrezol, and O. Leclerc, "Combining control electronics with SOA to equalize packet-to-packet power variations for optical 3R regeneration in optical networks at 10 Gbit/s," in *Proc. Opt. Fiber Commun. Conf.*, 2004, vol. 1, WD2.
- [19] A. A. M. Saleh, "Nonlinear models of travelling-wave optical amplifiers," *Electron. Lett.*, vol. 24, no. 14, pp. 835–837, Jul. 1988.
- [20] L. A. Coldren and S. W. Corzine, *Diode Lasers and Photonic Integrated Circuits*. New York: Wiley, 1995.
- [21] W. Kaplan, *Advanced Calculus*, 4th ed. New York: Addison-Wesley, 1991.
- [22] AmpSOA documentation, VPIsystems. Holmdel, NJ, 2005.
- [23] Z. Stanislaw, *Systems and Control*. New York: Oxford Univ. Press, 2003.

Scott B. Kuntze received the B.Sc.Eng. degree in mathematics and engineering from Queen's University, Kingston, ON, Canada, in 2002 and the M.A.Sc. degree in electrical engineering (photonics) from the University of Toronto, Toronto, ON, Canada, in 2004, where he is currently working toward the Ph.D. degree in photonics in the Department of Electrical and Computer Engineering.

He spent internships working in the Advanced Technology Investments department at Nortel Networks building next-generation photonic transceivers and switches from 2000 to 2001, and in the High Performance Optical Components division at Nortel studying semiconductor lasers using novel probing techniques in 2002. His current research interests include the robust analysis, design, and control of integrable active photonic devices using control theory.

Lacra Pavel (M'92–SM'04) received the Ph.D. degree in electrical engineering from Queen's University, Kingston, ON, Canada, in 1996, with a dissertation on nonlinear H-infinity control.

She spent a year at the Institute for Aerospace Research (NRC) in Ottawa as a NSERC Postdoctoral Fellow. From 1998 to 2002, she worked in the optical communications industry at the frontier between systems control, signal processing, and photonics. She joined the University of Toronto, Toronto, ON, Canada, in August 2002 as an Assistant Professor in Electrical and Computer Engineering Department. Her research interests include system control and optimization in optical networks, game theory, robust and H-infinity optimal control, and real-time control and applications.

Dr. Pavel served as Associate Editor, Member on the Program Committee of IEEE Control Applications Conference 2005; Associate Chair (Control) on the Program Committee of IEEE Canadian Conference of Electrical and Computer Engineering 2004. She is a member of CSS, ComSoc, LEOS, the Optical Society of America (OSA).

J. Stewart Aitchison (M'96–SM'00) received the B.Sc. (first-class hon.) and Ph.D. degrees from the Physics Department, Heriot-Watt University, Edinburgh, U.K., in 1984 and 1987, respectively. His dissertation research was on optical bistability in semiconductor waveguides.

From 1988 to 1990, he was a Postdoctoral Member of Technical Staff at Bellcore, Red Bank, NJ. His research interests were in high nonlinearity glasses and spatial optical solitons. He then joined the Department of Electronics and Electrical Engineering, University of Glasgow, Glasgow, U.K., in 1990 and was promoted to a personal chair as Professor of Photonics in 1999. His research was focused on the use of the half bandgap nonlinearity of III–V semiconductors for the realization of all-optical switching devices and the study of spatial soliton effects. He also worked on the development of quasi-phase matching techniques in III–V semiconductors, monolithic integration, optical rectification, and planar silica technology. His research group developed novel optical biosensors, waveguide lasers and photosensitive direct writing processes based around the use of flame hydrolysis deposited (FHD) silica. In 1996, he was the holder of a Royal Society of Edinburgh Personal Fellowship and carried out research on spatial solitons as a visiting researcher at CREOL, University of Central Florida. Since 2001, he has held the Nortel chair in Emerging Technology, in the Department of Electrical and Computer Engineering, University of Toronto, Toronto, ON, Canada. His research interests cover all-optical switching and signal processing, optoelectronic integration and optical biosensors. His research has resulted in seven patents, approximately 170 journal publications, and 200 conference publications. In 2004, he became the director of the Emerging Communications Technology Institute, University of Toronto.

Dr. Aitchison is a Fellow of the Optical Society of America and a Fellow of the Institute of Physics London.